HHS Public Access

Author manuscript

Cell Rep. Author manuscript; available in PMC 2024 July 16.

Published in final edited form as:

Cell Rep. 2024 June 25; 43(6): 114346. doi:10.1016/j.celrep.2024.114346.

Impaired islet function and normal exocrine enzyme secretion occur with low inter-regional variation in type 1 diabetes

Denise M. Drotar[1], **Ana Karen Mojica-Avila**[2,3,4], **Drew T. Bloss**[1], **Christian M. Cohrs**[2,3,4], **Cameron T. Manson**[1,5], **Amanda L. Posgai**[1], **MacKenzie D. Williams**[1], **Maigan A. Brusko**[1], **Edward A. Phelps**[5], **Clive H. Wasserfall**[1,6], **Stephan Speier**[2,3,4], **Mark A. Atkinson**[1,6,7,*]

[1]Department of Pathology, Immunology and Laboratory Medicine, University of Florida Diabetes Institute, Gainesville, FL 32610, USA

[2]Institute of Physiology, Faculty of Medicine, Technische Universität Dresden, Dresden, Germany

[3]Paul Langerhans Institute Dresden (PLID) of the Helmholtz Zentrum München at the University Clinic Carl Gustav Carus of Technische Universität Dresden, Helmholtz Zentrum München, Neuherberg, Germany

[4]German Center for Diabetes Research (DZD), München, Neuherberg, Germany

[5]J. Crayton Pruitt Family Department of Biomedical Engineering, University of Florida, Gainesville, FL, USA

[6]Department of Pediatrics, College of Medicine, University of Florida Diabetes Institute, Gainesville, FL, USA

[7]Lead contact

SUMMARY

Histopathological heterogeneity in the human pancreas is well documented; however, functional evidence at the tissue level is scarce. Herein, we investigate *in situ* glucose-stimulated islet and carbachol-stimulated acinar cell secretion across the pancreas head (PH), body (PB), and tail (PT) regions in donors without diabetes (ND; $n = 15$), positive for one islet autoantibody (1AAb+; $n = 7$), and with type 1 diabetes (T1D; <14 months duration, $n = 5$). Insulin, glucagon, pancreatic amylase, lipase, and trypsinogen secretion along with 3D tissue morphometrical features are comparable across regions in ND. In T1D, insulin secretion and beta-cell volume are significantly reduced within all regions, while glucagon and enzymes are unaltered. Beta-cell volume is lower despite normal insulin secretion in 1AAb+, resulting in increased volume-adjusted insulin

*Correspondence: atkinson@pathology.ufl.edu.

AUTHOR CONTRIBUTIONS

Conceptualization, S.S. and M.A.A.; methodology, D.M.D. and A.K.M.-A.; investigation, D.M.D., A.K.M.-A., D.T.B., C.M.C., and C.T.M.; writing – original draft, D.M.D., A.K.M.-A., and D.T.B.; writing – review & editing, D.M.D, A.K.M.-A., C.M.C., C.T.M., A.L.P., M.D.W., M.A.B., E.A.P., C.H.W., S.S., and M.A.A.; funding acquisition, E.A.P., S.S., and M.A.A.; supervision, M.A.B., C.H.W., S.S., and M.A.A.;

DECLARATION OF INTERESTS

The authors declare no competing interests.

SUPPLEMENTAL INFORMATION

Supplemental information can be found online at https://doi.org/10.1016/j.celrep.2024.114346.

secretion versus ND. Islet and acinar cell secretion in 1AAb+ are consistent across the PH, PB, and PT. This study supports low inter-regional variation in pancreas slice function and, potentially, increased metabolic demand in 1AAb+.

In brief

Drotar et al. investigate inter-regional variation in islet and acinar cell function using live pancreas slices from donors without and with type 1 diabetes (T1D). Endocrine and exocrine secretion are similar across the head, body, and tail regions. T1D insulin secretion is impaired, while exocrine secretion is preserved.

Graphical Abstract

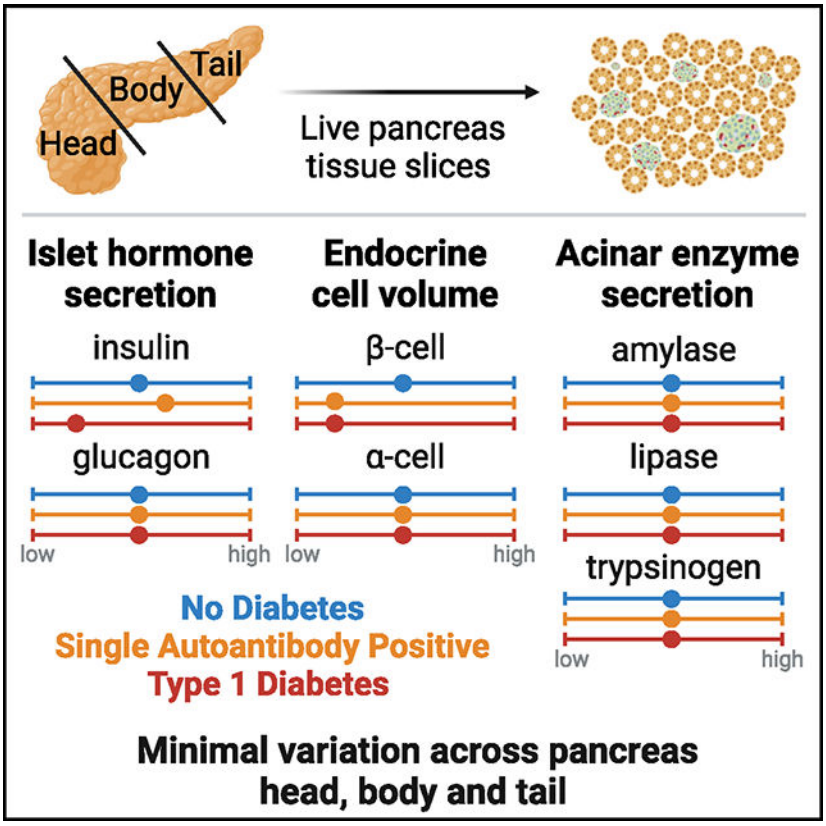

INTRODUCTION

In type 1 diabetes (T1D), islet infiltration is lobular yet intermittent.[1,2] Recent efforts have demonstrated that alpha cells[3–5] and the exocrine compartment[6–8] may also be impacted during T1D pathogenesis. Indeed, aberrant glucagon levels were described in individuals with T1D,[9–11] and hypoglycemia-induced alpha-cell failure was proposed as a possible mechanism.[3] Notably, overall pancreas weight/volume is decreased in individuals with T1D, those without diabetes who are positive for islet autoantibodies (AAb+), and healthy first-degree relatives of patients with T1D.[12–16] Serum trypsinogen and lipase levels are also significantly decreased, within the low end of the normal reference range, in individuals with

pre-T1D as well as in those with recent-onset and established T1D.[17,18] Whether this is due to a reduced number of acinar cells,[7] individual acinar cell size,[6] or an intrinsic functional defect is unclear.

Extensive characterization of pancreata from individuals with no diabetes (ND) has unveiled differences in islet size, cellular composition, and density across the three main regions of the organ.[19–22] Specifically, large islets contain increased proportions of alpha cells, whereas small islets are almost exclusively comprised of beta cells.[19] Alpha- and beta-cell frequencies are reduced in the pancreas head (PH) compared to the pancreas body (PB) and tail (PT) due to increased numbers of PP (pancreatic polypeptide)-secreting cells in the uncinate process within the PH.[21] Islet density is similar within the PH and PB yet significantly increased in the PT.[22] The functional relevance of these morphological differences across the organ is still unclear, and whether pancreatic heterogeneity plays a role in T1D development remains to be investigated.

Human pancreas tissue function is difficult to study, and most of our knowledge is based on systemic measurements of serological markers in response to standardized tests. Understanding of human islet biology and pathophysiology has increased dramatically in recent decades with improved access to human pancreas tissues via the Network for Pancreatic Organ Donors with Diabetes (nPOD),[23,24] the Human Pancreas Analysis Program, and the Integrated Islet Distribution Program.[25] Isolated islet preparations from ND donors are widely used to assess islet function yet lack information regarding the local microenvironment. Moreover, islet isolation from T1D pancreata is challenging and biased toward islets that survive the isolation process.[26] Biopsy studies (e.g., laparoscopically procured tissue from PT in DiViD) could provide a localized source of islets; however, such studies have been extremely limited by complications.[27,28] Alternative approaches, such as live tissue slice preparation, now enable investigation of islets within their tissue environment from T1D, AAb+, and ND donors.[29–32] Pancreas slices retain tissue architecture with islets surrounded by acinar cells,[33] preserved vasculature,[31,34] and extracellular matrix,[35] facilitating the investigation of the collective function of endocrine cells and acinar tissue simultaneously.

We hypothesized that the reported differences in islet density and composition among the three pancreas regions[20,21] might influence islet and acinar cell secretion. We thus performed an extensive functional study of the three pancreatic regions in humans by investigating the release of insulin, glucagon, amylase, lipase, and trypsinogen using live pancreas tissue slices. We characterized islet function and volume as well as acinar cell function, all averaged across 8–12 slices per region from the PH, PB, and PT of each donor: 15 ND, 7 single AAb+ (1AAb), and 5 recent-onset T1D (disease duration <14 months) (Table S1; Figures S1A–S1G).

RESULTS

Similar hormone secretion, islet composition, and enzyme secretion across PH, PB, and PT in human ND pancreas

Hormone release was assessed in freshly prepared tissue slices from the PH, PB, and PT of 15 ND donors. Glucose stimulation of live pancreas slices elicited the expected two-phase insulin secretion kinetics in all three regions at both medium (5.5 mM) and high (11.1 mM) glucose concentrations, referred to as 5.5G and 11.1G, respectively, as well as following membrane depolarization (30 mM KCl) (Figure 1A). Quantifying insulin responsiveness to all applied stimuli (glucose or KCl) showed a similar secretion output in slices prepared from the different regions (Figures 1B–1D). Glucagon secretion was measured at the same time points as insulin and normalized to the 5.5G step in order to investigate both the stimulatory and suppressive effects of glucose (Figure 1E). Glucagon release in response to decreases in glucose concentration (5.5G to 1G or 11.1G to 1G) and KCl were comparable across all regions (Figures 1F–1I), with no regional difference in the suppression of glucagon release upon high glucose infusion (Figure 1G).

After functional assessment, we employed whole-slice 3D morphometric analysis to quantify total insulin and glucagon volumes from islets, clusters, and single cells in 7 ND pancreata. Overall, slice tissue volumes used for perifusion and 3D morphometric quantification were comparable across the three regions from ND (Figure 1J). Whole-slice 3D morphometric analysis demonstrated similar islet density and endocrine volume across the PH, PB, and PT in ND (Figures 1K–1N). Insulin contributed 70%–80% to the observed endocrine volume in all ND pancreas regions (Figure 1O).

We also investigated acinar cell secretory function using adjacent slices from the same donors and regions, comparing pancreatic amylase, lipase, and trypsinogen release. Under basal conditions, similar secretion of all three enzymes was observed across the PH, PB, and PT (Figures 1P–1R). Upon stimulation with 10 μM carbachol, a widely used stimulus of acinar cell secretion,[33] secretion of all pancreatic enzymes increased ~10-fold, yet stimulated enzyme levels did not significantly differ across regions (Figures 1S–1U). Altogether, these data indicate that in *ex vivo* pancreas slices, islets and acinar cells have similar secretion responses, independent of the region of origin within the ND pancreas.

Diminished insulin and normal glucagon secretion across all pancreatic regions in recent-onset T1D

We next investigated whether T1D might differentially affect islet cell secretion within the PH, PB, and PT. Insulin responses in slices from the 1AAb+ group were similar to ND in all pancreas regions (Figures 2A–2I, S2A–S2E, orange lines, and S3A–S3E). In comparison to control and 1AAb+ groups, glucose-stimulated insulin secretion (GSIS) was dramatically diminished in all 5 recent-onset T1D cases investigated, with loss of the typical two-phase insulin response[3,29] (Figures 2A–2I and S2A–S2E, red lines). Specifically, two donors had undetectable insulin secretion (Figures S3F–S3J). Overall, there were no significant differences in insulin responsiveness across the regions in T1D. Furthermore, upon baseline normalization, insulin responses to 5.5G were completely lost in slices from

all pancreas regions. Interestingly, 2/5 cases with T1D still showed weak 11.1G peaks (Figures 2D–2H and S3I). Moreover, some slices from 3 donors with recent-onset T1D exhibited a near-normal response to KCl (Figures 2D–2F and 2I), but the responsive region varied for each case (Figure S3J). Altogether, these data suggest reduced glucose sensitivity and preserved insulin secretion capacity in these donors.

Glucagon secretion was measured in the same slices (Figures 2J–2O). Absolute amounts of glucagon release were variable (Figures 2J–2L); however, after normalization to the 5.5G baseline, glucagon responses to changes in glucose concentrations did not differ significantly across disease groups (Figures 2M–2S and S2F–S2K) or pancreatic regions (Figures S3K–S3V).

Preserved acinar cell function at T1D onset

Similar to ND, we measured pancreatic enzyme release in slices from each region of 1AAb+ and recent-onset T1D groups. Basal release of pancreatic amylase, lipase, and trypsinogen was comparable in slices from 1AAb+, T1D, and ND pancreata across all regions (Figures 3A–3C). Following carbachol stimulation, enzyme secretion increased ~10-fold across all regions in the 1AAb+ and T1D groups (Figures 3D–3F), with a decreased lipase response in the PH in the T1D group (Figure 3E). The stimulation index was similar across disease groups and pancreatic regions (Figures 3G–3I).

Decreased endocrine and beta-cell volume across the pancreas at T1D onset

To assess the relationship between endocrine mass and function at T1D onset, we performed a 3D morphometric analysis of perifused slices. Slices prepared from PH, PB, and PT of 7 ND, 5 1AAb+, and 5 recent-onset T1D pancreata had similar overall volumes (Figure 4A). The endocrine cell volume (sum of insulin and glucagon) was significantly decreased in both 1AAb+ and T1D (Figure 4B) due to a significant reduction of beta-cell volume together with normal alpha-cell volume in the PH and PB (Figures 4C and 4D). Islet density appeared to be lower in 3 cases with T1D as compared to ND but did not reach statistical significance (PH, $p = 0.2290$; PB, $p = 0.3115$; PT, $p = 0.3666$) (Figure 4E). While total endocrine cell volume was not significantly reduced in the PT, we found a reduced beta-to-alpha cell ratio in the PT of donors with T1D (Figures 4F–4H).

Next, we used the volumetric data to normalize hormone secretion to investigate insulin secretion in the remaining beta-cell volume within the slices (Figures 4I–4K). In all pancreas regions, beta-cell volume-normalized insulin secretion was diminished in T1D slices, particularly upon 11.1G stimulation (Figures 4L–4O). In contrast, with beta-cell volume decreased in 1AAb+ slices (Figure 4C), while overall secretion was preserved (Figures 2A–2I), the volume-adjusted insulin secretion appeared to be amplified in some 1AAb+ slices when compared to ND (Figures 4I–4K). Interestingly, one subject with 1AAb+ showed an inverted pattern of insulin secretion at 5.5G stimulation, with an increase during the second phase of insulin release. Importantly, none of the 1AAb+ cases investigated herein showed signs of dysglycemia, as serum HbA1c and C-peptide levels were normal (Figure S1). We also used alpha-cell volumes to normalize glucagon secretion within the same slices. When adjusted to the glucagon+ alpha-cell volume, glucagon secretion was consistent across all

regions in ND and 1AAb+ (Figures 4P–4R). PT slices of recent-onset T1D showed slightly increased alpha-cell volume-normalized glucagon release (Figure 4R) but did not reach significance in our analysis (Figures 4S–4V).

DISCUSSION

Herein, we performed an extensive functional study on islet and acinar cells across the three human pancreas regions in ND, 1AAb+, and recent-onset T1D. To date, we are aware of only one study that compared GSIS in isolated islets from the PH + PB versus the PT.[20] Our results from living tissue slices confirm that two-phase insulin release is similar across these pancreatic regions in ND,[29,36] finding analogous results for glucagon and pancreatic enzyme secretion in this comprehensive investigation of endocrine and exocrine function within the same tissues. Specifically, despite known developmental, morphological, and histological differences across the main pancreatic regions (e.g., proportions of beta, alpha, delta, or PP cells),[20–22] we observed similar hormone secretion and enzyme release across the PH, PB, and PT of ND.

3D morphometrical analysis indicated similar endocrine cell mass, composition, and islet density across regions. These results differ from previous histologic studies on ND human pancreata reporting increased islet density in the PT and diminished frequencies of alpha and beta cells in PH.[20,21] These disparities could be explained by human donor variability or by differences in scale. Histological cross-sections are thin (4–5 μM) but cover a large tissue area (80–100 mm^2).[37] Using tissue slices of 120 μm thickness, we have evaluated a smaller surface area but increased volume (~1 mm^3/slice). A recent 3D whole-pancreas imaging study reported uniform distribution of insulin volumes across pancreas regions.[38] Nevertheless, such studies are scarce, highlighting the need to improve our understanding of whole-pancreas islet distribution in 2D versus 3D.

We hypothesized that during T1D pathogenesis, some regions might exhibit a greater degree of dysfunction than others based on the well-recognized phenomenon of inconsistent, lobular patterns of immune infiltration and islet destruction.[2] While limited to 1AAb+ cases (six GAD+ [glutamic acid decarboxylase] and one mIAA+ [insulin]), this is a leading-edge study investigating islet and acinar cell function in slices from AAb+ cases, who are considered to have increased T1D risk.[39,40] Absolute and baseline-normalized insulin secretion from 1AAb+ slices were similar to ND in all regions. Insulin volume, quantified by 3D morphometry of perifused slices, was significantly decreased in 1AAb+ PH and PB; hence, the adjusted insulin release was increased in all regions from this group, perhaps suggesting an adaptation to a higher workload to maintain glycemic control. One 1AAb+ case showed increased second-phase insulin release when stimulated with 5.5G, suggesting that changes in secretion dynamics might precede functional beta-cell failure. Interestingly, it was previously shown that some individuals with 1AAb+ present signs of beta-cell dysfunction years before T1D diagnosis,[41] but whether or when our 1AAb+ donors would have developed T1D is unknown.

In recent-onset T1D (<14 month duration), we observed a dramatic loss of GSIS across all regions, concomitant with significantly reduced insulin+ beta-cell volume in the PH

and PB. While insulin volume was not significantly decreased in the PT, significant changes in the alpha- and beta-cell mass proportions were observed in T1D versus ND slices. Interestingly, the KCl response was preserved in 3/5 cases, suggesting a defect in glucose responsiveness rather than insulin production, confirming previous observations.[29] Nevertheless, beta-cell volume-normalized insulin release was dramatically reduced in all regions for most donors with T1D, suggesting functional impairment of the remaining beta-cell mass. This finding corroborates previous human studies using T1D slices[29] but differs from those in isolated islets, where residual beta-cells retained features of regulated insulin secretion.[4,5] These observations could be driven by differences in tissue preparation (e.g., mechanical and chemical stressors during isolation, recovery culture times, potential selectivity bias toward intact islets), stimuli (amino acids or IBMX [isobutylmethylxanthine] versus glucose), and analysis approach (normalization to islet numbers/islet equivalent versus baseline/morphometry).

Within these same samples, we found no differences in glucagon secretion or alpha-cell volumes across the PH, PB, and PT of ND pancreas, nor across the ND, 1AAb+, and T1D groups, suggesting that alpha-cell volume and function are preserved at T1D onset. This contrasts with previous reports of dysregulated glucagon secretion from alpha cells within tissue slices[3] and isolated human islets.[4,5] Besides the described methodological differences, perhaps most noteworthy is the difference in donor age and diabetes duration—these previously published studies[3–5] investigated islet functionality in older donors with established T1D (up to 30 years duration), while most of our donors were diagnosed at demise.

The contribution of the exocrine compartment in T1D has more recently gained interest, sparked by observations of decreased pancreas size in T1D but also in AAb+ and first-degree relatives.[12–14,16] Circulating levels of pancreatic amylase, lipase, and trypsinogen[17,18] and fecal elastase-1 levels[42,43] are significantly reduced even before T1D diagnosis, but whether this results from an acinar cell functional deficit is not fully understood.[44] We evaluated acinar cell secretion in ND, 1AAb+, and recent-onset T1D tissues and found no significant differences in baseline or carbachol-stimulated secretion of pancreatic enzymes across groups or pancreas regions. These results suggest that acinar cell secretory function might not be affected and, rather, point to reduced pancreas organ mass—which is well documented in established, recent-onset, and pre-T1D[12,13,16]—and reduced acinar cell numbers[7] as the likely reasons for lower pancreatic enzyme levels during T1D progression.[17,18] However, factors that cannot be accounted for within our model, such as tissue innervation, vascularization, and perifusion, might play a role in the production and release of pancreatic enzymes *in vivo*.

Taken together, our data demonstrate that islet and acinar cell secretion profiles were comparable between the PH, PB, and PT. Insulin secretion was dramatically impaired across the organ in recent-onset T1D, while alpha- and acinar cell secretion were unaltered in 1AAb+ and T1D. Further studies are needed on pancreas slices from rare donors with pre-T1D (i.e., ≥2AAb+) to characterize the progressive loss of islet function across disease stages. Additionally, such functional studies should be expanded to cover larger tissue areas and volumes within the pancreas, in combination with high-content tissue imaging or spatial

gene expression analyses, for a better understanding of the complete architecture of T1D pathogenesis.

Limitations of the study

While we completed an extensive investigation of islet and acinar cell secretion across the pancreatic regions in ND, 1AAb+, and T1D, this poses certain limitations. Live tissue slices were prepared from one cross-section within each region and therefore might not fully reflect biology or pathophysiology across the entire region. To overcome this, we prepared 40 ± 15 slices from several tissue blocks within each cross-section, and 8–12 slices were randomly selected for functional assays to provide an impartial representation of that region. We were also limited in the number of pancreata available for research; therefore, exact case matching (for age, sex, BMI, HLA [human leukocyte antigen]) was not possible. A scarcity of AAb+ donors restricted our ability to perform investigations on tissues from individuals with a high risk of developing T1D. For this reason, we conducted these studies on every pancreas from the ND, AAb+, or T1D group received by nPOD within the past 3 years and only excluded cases with exceptional medical histories (e.g., endocrine pancreas tumors, or monogenic diabetes including MODY [maturity-onset diabetes of the young]). Of course, organ donor tissues can only provide cross-sectional information. While clinical history is provided for each donor, and the medical chart contains an array of information used for donor characterization, further investigations and additional diagnoses that might facilitate specific research questions (e.g., metabolic phenotyping with glucose or mixed-meal tolerance tests or detailed testing for exocrine disease) are not always possible. Despite these limitations, the organized procurement of transplant-grade pancreata provides an invaluable resource for studying the human pancreas, and we believe that this study gives unique insights into islet and acinar cell function in the three anatomical regions of the pancreas as well as the early phases of T1D pathogenesis.

STAR★METHODS

RESOURCE AVAILABILITY

Lead contact—Further information and requests for resources and reagents should be directed to and will be fulfilled by the lead contact, Mark A. Atkinson (atkinson@pathology.ufl.edu).

Materials availability—This study did not generate new unique reagents or materials.

Data and code availability

- All data reported in this paper will be shared by the lead contact upon request.
- This paper does not report original code.
- Any additional information required to reanalyze the data reported in this work paper is available from the lead contact upon request.

EXPERIMENTAL MODEL AND STUDY PARTICIPANT DETAILS

All procedures were performed according to the established standard operating procedures of the nPOD/OPPC and approved by the University of Florida Institutional Review Board (IRB201600029) and the United Network for Organ Sharing (UNOS) according to federal guidelines, with informed consent obtained from each donor's legal representative. Pancreas tissue from human donors with or without T1D was procured from the nPOD program at the University of Florida (RRID: SCR_014641, https://www.jdrfnpod.org). For each donor, a medical chart review was performed, and C-peptide was measured, with T1D diagnosed according to the guidelines established by the American Diabetes Association (ADA). Demographic data, hospitalization duration, and organ transport time were obtained from hospital records. Donor pancreata were recovered, placed in transport media on ice, and shipped via organ courier to the University of Florida. The tissue was processed by a licensed pathology assistant. Detailed donor information is listed in Table S1.

METHOD DETAILS

Living pancreas tissue slice preparation—Fresh, living tissue slices from organ donor pancreata were prepared as previously described.[29] Briefly, cross-sections from the PH, PB, and PT regions of 27 human pancreata (Table S1) were freshly obtained from nPOD (https://npod.org) and placed into separate 100 mm dishes containing ECS (125 mM NaCl, 26 mM $NaHCO_3$, 10 mM HEPES, 3 mM glucose, 2.5 mM KCl, 2 mM $CaCl_2$, 1.25 mM NaH_2PO_4, 1 mM $MgCl_2$, pH 7.4) supplemented with aprotinin (25 KIU/mL). Small tissue pieces approximately 0.5 cm^3 in size were cut from the larger cross sections, and any remaining connective, fibrotic, or adipose tissue was removed before embedding the pieces in low-melting point agarose (3.8%). The agarose solidified at 4°C–8°C and the resulting tissue blocks were mounted onto the specimen holder of a semi-automated vibratome. The tissue blocks were sliced at a thickness of 120 μm, speed of 0.1–0.2 mm/s, amplitude of 1 mm, and angle of 15°. Slices were collected in separate dishes containing ECS with aprotinin. After slices from all regions were prepared, they were transferred to dishes containing Low Glucose DMEM (Dulbecco's Modified Eagles Medium) supplemented with 10% FBS, antibiotic-antimycotic solution (1:100 dilution), and 25 KIU/mL aprotinin, and placed in an incubator set at 28°C with 5% CO_2 for overnight resting.

Dynamic perifusion assay for insulin and glucagon secretion measurement—Tissue slices were placed in 3mM glucose containing DMEM media supplemented with 3.2 g/L $NaHCO_3$, 1.11 g/L HEPES, 0.11 g/L sodium pyruvate, 4 mM L-glutamine, pH 7.4, 0.1% BSA and 25 KIU/mL aprotinin for 2 h, gently rocking. After the 2-h resting period, slices from the PH, PB, and PT regions were loaded into separate perifusion chambers (4 slices/chamber/region) and connected to a perifusion system. Tissue slices were perifused at a flow rate of 100 μL/min at 37°C, and the perifusate was collected in 96-well plates at 2-min intervals. The slices were first flushed with media containing 3 mM glucose for 60 min to wash out accumulated hormones and enzymes, and then subjected to a series of glucose challenges – 10 min of media with 1 mM glucose, 20 min with 5.5 mM glucose, 20 min with 1 mM glucose, 20 min with 11.1 mM glucose, 20 min with 1 mM glucose, 10 min with 11.1 mM glucose and 30 mM KCl, and 10 min with 1 mM glucose. Perifusate

samples were stored at −20°C until measurement of insulin and glucagon with commercially available ELISA kits.

After perifusion, slices were removed from the chambers and fixed in 4% paraformaldehyde for 30 min, then washed in PBS for 5 min. The slices were then transferred into 5 mL tubes filled with PBS with azide and stored at 4°C until shipment to the Paul Langerhans Institute Dresden for 3D morphometric analysis.

Assessment of pancreatic amylase, lipase, and trypsinogen release—Five slices from the PH, PB, and PT regions were incubated in 3 mM glucose containing DMEM media, supplemented with aprotinin on an orbital shaker (15–20 rpm) at 37°C for 1 h. After the 1-h resting period, slices were transferred to a 24-well plate with 500 μL of fresh media in each well. Basal secretion samples were collected after a 30-min incubation at 37°C on an orbital shaker. Slices were then stimulated with 10 μM carbachol for 30 min at 37°C on an orbital shaker. After the stimulation step the supernatants were collected, and the slices were placed into 500 mL 3 mM DMEM with 3% Triton X-100 for the assessment of total slice enzyme content. All samples were stored at −20°C until amylase, lipase and trypsinogen measurement using commercially available ELISA and RIA kits.

Immunofluorescent staining and whole slice 3D imaging—Whole slices were immersed in a blocking solution (GSDB) containing 0.3% Triton X-100 (1% goat serum, 0.3% Triton X-100, 900 mM NaCl, and 40 mM sodium phosphate buffer in deionized water with a pH of 7.4) and stained using primary antibodies targeting insulin (1:10 dilution) and glucagon (1:2000 dilution) for 24–48 h at 4°C with gentle shaking. After primary antibody incubation, the slices were washed three times for at least 30 min each with PBS. Subsequently, the slices were incubated with secondary antibodies: Alexa Fluor 488 goat anti-guinea pig (1:200 dilution) for insulin, Alexa Fluor 633 goat anti-mouse (1:200 dilution) for glucagon, and DAPI (2.5 mg/ml) overnight at 4°C with gentle shaking. Following secondary antibody and DAPI incubation, the slices were washed three times for at least 30 min. Slices were then stored in PBS at 4°C in the dark until imaging.

Stained slices were mounted underneath a glass coverslip, submerged in PBS (pH 7.4), and imaged in their entirety using an up-right laser scanning confocal microscope (TCS SP8 SMD, Leica) equipped with a water-immersion 20x high NA objective lens and a motorized stage. Single tiles were imaged as previously described,[29] at a resolution of 0.75 × 0.75 mm, with a tile overlap of 15% and a stack separation of 2.5 mm. DAPI and fluorescent antibodies were excited at 405nm, 488nm and 633nm, and detected at 405–510nm (for DAPI), 490–560nm (insulin), and 638–755nm (glucagon), respectively.

3D morphometric analysis of insulin and glucagon volumes—Tilescans were stitched using the built-in stitching function of the Las X Life Science Microscope Software Platform. Data quantification was semi-automatically conducted using a customized FIJI toolset, as previously described.[26] Briefly, total slice area and individual endocrine objects (defined as those positive for at least one hormone stain) were manually contoured on a maximum intensity projection, and regions of interest (ROIs) were saved separately. For individual endocrine particles, regions were cropped from the stitched tilescan, followed

by subtraction of the 488 channel from the 546 channel and removal of the 546 channel from the 633 channel to account for channel bleed. Images were then split by color, contrast-enhanced (CLAHE), involving median filtering (3 × 3 × 1) and conversion to binary (IJ_IsoData).

Further processing included hole filling in 3D, size opening (limited to 500 μm^3), and volume analysis (Euler connectivity: C26) using MorphoLibJ.[45] The total slice volume was calculated by adding each channel of the original tilescan and cropping it using the previously contoured total slice ROI. Additional steps included median filtering (3 × 3 × 1), mask generation for nearby points (within a distance of 10.0 μm, threshold of 12.75), removal of dark and bright outliers, hole filling, 3D volume closing (cube, 3 × 3 × 1), and volume analysis for endocrine objects using MorphoLibJ.[45]

QUANTIFICATION AND STATISTICAL ANALYSIS

No specific statistical methods were used to predetermine sample size due to no ability to predict sample availability. All results are presented as mean ± SEM. Logarithmic transformation was used to ensure normal data distribution prior to conducting statistical analysis. The significance of the differences between groups was analyzed with one-way ANOVA followed by multiple comparisons for differences across the regions within a disease group, and two-way ANOVA for simultaneous comparisons of regions and disease groups, as indicated in the figure legends. p values <0.05 were considered statistically significant. All statistical analyses were performed using GraphPad Prism Software version 9.

ADDITIONAL RESOURCES

Data Portal of the Network for Pancreatic Organ Donors with Diabetes, contains detailed information about each donor tissue used in this study: https://portal.jdrfnpod.org/.

Supplementary Material

Refer to Web version on PubMed Central for supplementary material.

ACKNOWLEDGMENTS

We would like to thank the nPOD Administrative and Organ Processing and Pathology Core teams, respectively, led by Drs. Mingder Yang and Irina Kusmartseva for assisting with organ procurement and processing. This work was supported by the National Institutes of Health (NIH) R01-DK123292 and R01-DK131059, the DFG Collaborative Research Centre/Transregio 127, the DFG — International Research Training Group 2251, JRDF grant 2-SRA-2019-696-S-B, the Paul Langerhans Institute Dresden (PLID) of the Helmholtz Zentrum Mu€nchen at the University Clinic Carl Gustav Carus of Technische Universität Dresden, and the German Ministry for Education and Research to the German Centre for Diabetes Research. We also acknowledge the support of NPOD (RRID: SCR_014641), a collaborative T1D research project sponsored by JDRF (nPOD: 5-SRA-2018-557-Q-R), The Leona M. and Harry B. Helmsley Charitable Trust (grants 2018PG-T1D053, 2018PG-T1D060, and 2015PG-T1D052), and the Diabetes Research Institute Foundation. The content and views expressed are the responsibility of the authors and do not necessarily reflect the official view of nPOD. Organ procurement organizations partnering with nPOD to provide research resources are listed at http://www.jdrfnpod.org//for-partners/npod-partners. Finally, we wholeheartedly thank the donors and their families for their invaluable contribution to science. The graphical abstract was created with BioRender.com.

REFERENCES

1. Rodriguez-Calvo T, Ekwall O, Amirian N, Zapardiel-Gonzalo J, and von Herrath MG (2014). Increased immune cell infiltration of the exocrine pancreas: a possible contribution to the pathogenesis of type 1 diabetes. Diabetes 63, 3880–3890. 10.2337/db14-0549. [PubMed: 24947367]
2. Rodriguez-Calvo T, Suwandi JS, Amirian N, Zapardiel-Gonzalo J, Anquetil F, Sabouri S, and von Herrath MG (2015). Heterogeneity and Lobularity of Pancreatic Pathology in Type 1 Diabetes during the Pre-diabetic Phase. J. Histochem. Cytochem. 63, 626–636. 10.1369/0022155415576543. [PubMed: 26216138]
3. Panzer JK, and Caicedo A (2021). Targeting the Pancreatic α-Cell to Prevent Hypoglycemia in Type 1 Diabetes. Diabetes 70, 2721–2732. 10.2337/dbi20-0048. [PubMed: 34872936]
4. Doliba NM, Rozo AV, Roman J, Qin W, Traum D, Gao L, Liu J, Manduchi E, Liu C, Golson ML, et al. (2022). a Cell dysfunction in islets from nondiabetic, glutamic acid decarboxylase autoantibody-positive individuals. J. Clin. Invest. 132, e156243. 10.1172/JCI156243. [PubMed: 35642629]
5. Brissova M, Haliyur R, Saunders D, Shrestha S, Dai C, Blodgett DM, Bottino R, Campbell-Thompson M, Aramandla R, Poffenberger G, et al. (2018). α Cell Function and Gene Expression Are Compromised in Type 1 Diabetes. Cell Rep. 22, 2667–2676. 10.1016/j.cel-rep.2018.02.032. [PubMed: 29514095]
6. Tang X, Kusmartseva I, Kulkarni S, Posgai A, Speier S, Schatz DA, Haller MJ, Campbell-Thompson M, Wasserfall CH, Roep BO, et al. (2021). Image-Based Machine Learning Algorithms for Disease Characterization in the Human Type 1 Diabetes Pancreas. Am. J. Pathol. 191, 454–462. 10.1016/j.ajpath.2020.11.010. [PubMed: 33307036]
7. Wright JJ, Saunders DC, Dai C, Poffenberger G, Cairns B, Serreze DV, Harlan DM, Bottino R, Brissova M, and Powers AC (2020). Decreased pancreatic acinar cell number in type 1 diabetes. Diabetologia 63, 1418–1423. 10.1007/s00125-020-05155-y. [PubMed: 32388592]
8. Kusmartseva I, Beery M, Hiller H, Padilla M, Selman S, Posgai A, Nick HS, Campbell-Thompson M, Schatz DA, Haller MJ, et al. (2020). Temporal Analysis of Amylase Expression in Control, Autoantibody-Positive, and Type 1 Diabetes Pancreatic Tissues. Diabetes 69, 60–66. 10.2337/db19-0554. [PubMed: 31597639]
9. Brown RJ, Sinaii N, and Rother KI (2008). Too much glucagon, too little insulin: time course of pancreatic islet dysfunction in new-onset type 1 diabetes. Diabetes Care 31, 1403–1404. 10.2337/dc08-0575. [PubMed: 18594062]
10. Arbelaez AM, Xing D, Cryer PE, Kollman C, Beck RW, Sherr J, Ruedy KJ, Tamborlane WV, Mauras N, Tsalikian E, et al. (2014). Blunted glucagon but not epinephrine responses to hypoglycemia occurs in youth with less than 1 yr duration of type 1 diabetes mellitus. Pediatr. Diabetes 15, 127–134. 10.1111/pedi.12070. [PubMed: 23992543]
11. Diabetes Research in Children Network DirecNet Study Group; Tsalikian E, Tamborlane W, Xing D, Becker DM, Mauras N, Fiallo-Scharer R, Buckingham B, Weinzimer S, Steffes M, et al. (2009). Blunted Counter-regulatory Hormone Responses to Hypoglycemia in Young Children and Adolescents With Well-Controlled Type 1 Diabetes. Diabetes Care 32, 1954–1959. 10.2337/dc08-2298. [PubMed: 19675205]
12. Campbell-Thompson ML, Kaddis JS, Wasserfall C, Haller MJ, Pugliese A, Schatz DA, Shuster JJ, and Atkinson MA (2016). The influence of type 1 diabetes on pancreatic weight. Diabetologia 59, 217–221. 10.1007/s00125-015-3752-z. [PubMed: 26358584]
13. Campbell-Thompson ML, Filipp SL, Grajo JR, Nambam B, Beegle R, Middlebrooks EH, Gurka MJ, Atkinson MA, Schatz DA, and Haller MJ (2019). Relative Pancreas Volume Is Reduced in First-Degree Relatives of Patients With Type 1 Diabetes. Diabetes Care 42, 281–287. 10.2337/dc18-1512. [PubMed: 30552130]
14. Campbell-Thompson M, Rodriguez-Calvo T, and Battaglia M (2015). Abnormalities of the Exocrine Pancreas in Type 1 Diabetes. Curr. Diab. Rep. 15, 79. 10.1007/s11892-015-0653-y. [PubMed: 26318606]
15. Williams AJK, Thrower SL, Sequeiros IM, Ward A, Bickerton AS, Triay JM, Callaway MP, and Dayan CM (2012). Pancreatic volume is reduced in adult patients with recently diagnosed type 1 diabetes. J. Clin. Endocrinol. Metab. 97, E2109–E2113. 10.1210/jc.2012-1815. [PubMed: 22879632]

16. Campbell-Thompson M, Wasserfall C, Montgomery EL, Atkinson MA, and Kaddis JS (2012). Pancreas organ weight in individuals with disease-associated autoantibodies at risk for type 1 diabetes. JAMA 308, 2337–2339. 10.1001/jama.2012.15008.

17. Ross JJ, Wasserfall CH, Bacher R, Perry DJ, McGrail K, Posgai AL, Dong X, Muir A, Li X, Campbell-Thompson M, et al. (2021). Exocrine Pancreatic Enzymes Are a Serological Biomarker for Type 1 Diabetes Staging and Pancreas Size. Diabetes 70, 944–954. 10.2337/db20-0995. [PubMed: 33441381]

18. Li X, Campbell-Thompson M, Wasserfall CH, McGrail K, Posgai A, Schultz AR, Brusko TM, Shuster J, Liang F, Muir A, et al. (2017). Serum Trypsinogen Levels in Type 1 Diabetes. Diabetes Care 40, 577–582. 10.2337/dc16-1774. [PubMed: 28115475]

19. Bonner-Weir S, Sullivan BA, and Weir GC (2015). Human Islet Morphology Revisited: Human and Rodent Islets Are Not So Different After All. J. Histochem. Cytochem. 63, 604–612. 10.1369/0022155415570969. [PubMed: 25604813]

20. Wang X, Misawa R, Zielinski MC, Cowen P, Jo J, Periwal V, Ricordi C, Khan A, Szust J, Shen J, et al. (2013). Regional differences in islet distribution in the human pancreas–preferential beta-cell loss in the head region in patients with type 2 diabetes. PLoS One 8, e67454. 10.1371/journal.pone.0067454. [PubMed: 23826303]

21. Wang X, Zielinski MC, Misawa R, Wen P, Wang T-Y, Wang C-Z, Witkowski P, and Hara M (2013). Quantitative Analysis of Pancreatic Polypeptide Cell Distribution in the Human Pancreas. PLoS One 8, e55501. 10.1371/journal.pone.0055501. [PubMed: 23383206]

22. Savari O, Zielinski MC, Wang X, Misawa R, Millis JM, Witkowski P, and Hara M (2013). Distinct function of the head region of human pancreas in the pathogenesis of diabetes. Islets 5, 226–228. 10.4161/isl.26432. [PubMed: 24045229]

23. Campbell-Thompson M (2015). Organ donor specimens: What can they tell us about type 1 diabetes? Pediatr. Diabetes 16, 320–330. 10.1111/pedi.12286. [PubMed: 25998576]

24. Campbell-Thompson M, Wasserfall C, Kaddis J, Albanese-O'Neill A, Staeva T, Nierras C, Moraski J, Rowe P, Gianani R, Eisenbarth G, et al. (2012). Network for Pancreatic Organ Donors with Diabetes (nPOD): developing a tissue biobank for type 1 diabetes. Diabetes. Metab. Res. Rev. 28, 608–617. 10.1002/dmrr.2316. [PubMed: 22585677]

25. Brissova M, Niland JC, Cravens J, Olack B, Sowinski J, and Evans-Molina C (2019). The Integrated Islet Distribution Program Answers the Call for Improved Human Islet Phenotyping and Reporting of Human Islet Characteristics in Research Articles. Diabetes 68, 1363–1365. 10.2337/dbi19-0019. [PubMed: 31092479]

26. Lyon J, Manning Fox JE, Spigelman AF, Kim R, Smith N, O'Gorman D, Kin T, Shapiro AMJ, Rajotte RV, and MacDonald PE (2016). Research-Focused Isolation of Human Islets From Donors With and Without Diabetes at the Alberta Diabetes Institute IsletCore. Endocrinology 157, 560–569. 10.1210/en.2015-1562. [PubMed: 26653569]

27. Krogvold L, Edwin B, Buanes T, Ludvigsson J, Korsgren O, Hyöty H, Frisk G, Hanssen KF, and Dahl-Jørgensen K (2014). Pancreatic biopsy by minimal tail resection in live adult patients at the onset of type 1 diabetes: experiences from the DiViD study. Diabetologia 57, 841–843. 10.1007/s00125-013-3155-y. [PubMed: 24429579]

28. Krogvold L, Skog O, Sundström G, Edwin B, Buanes T, Hanssen KF, Ludvigsson J, Grabherr M, Korsgren O, and Dahl-Jørgensen K (2015). Function of Isolated Pancreatic Islets From Patients at Onset of Type 1 Diabetes: Insulin Secretion Can Be Restored After Some Days in a Nondiabetogenic Environment In Vitro: Results From the DiViD Study. Diabetes 64, 2506–2512. 10.2337/db14-1911. [PubMed: 25677915]

29. Panzer JK, Hiller H, Cohrs CM, Almaça J, Enos SJ, Beery M, Cechin S, Drotar DM, Weitz JR, Santini J, et al. (2020). Pancreas tissue slices from organ donors enable in situ analysis of type 1 diabetes pathogenesis. JCI Insight 5, e134525. 10.1172/jci.insight.134525. [PubMed: 32324170]

30. Marciniak A, Cohrs CM, Tsata V, Chouinard JA, Selck C, Stertmann J, Reichelt S, Rose T, Ehehalt F, Weitz J, et al. (2014). Using pancreas tissue slices for in situ studies of islet of Langerhans and acinar cell biology. Nat. Protoc. 9, 2809–2822. 10.1038/nprot.2014.195. [PubMed: 25393778]

31. Mateus Gonc¸alves L, and Almaça J (2020). Functional Characterization of the Human Islet Microvasculature Using Living Pancreas Slices. Front. Endocrinol. 11, 602519. 10.3389/fendo.2020.602519.

32. Cohrs CM, Chen C, Atkinson MA, Drotar DM, and Speier S (2024). Bridging the Gap: Pancreas Tissue Slices From Organ and Tissue Donors for the Study of Diabetes Pathogenesis. Diabetes 73, 11–22. 10.2337/dbi20-0018. [PubMed: 38117999]
33. Liang T, Dolai S, Xie L, Winter E, Orabi AI, Karimian N, Cosen-Binker LI, Huang Y-C, Thorn P, Cattral MS, and Gaisano HY (2017). Ex vivo human pancreatic slice preparations offer a valuable model for studying pancreatic exocrine biology. J. Biol. Chem. 292, 5957–5969. 10.1074/jbc.M117.777433. [PubMed: 28242761]
34. Mateus Gonçalves L, Fahd Qadir MM, Boulina M, Makhmutova M, Pereira E, and Almac a, J. (2023). Pericyte dysfunction and impaired vasomotion are hallmarks of islets during the pathogenesis of type 1 diabetes. Cell Rep. 42, 112913. 10.1016/j.celrep.2023.112913. [PubMed: 37531253]
35. Santini-González J, Simonovich JA, Castro-Gutiérrez R, González-Vargas Y, Abuid NJ, Stabler CL, Russ HA, and Phelps EA (2021). In vitro generation of peri-islet basement membrane-like structures. Biomaterials 273, 120808. 10.1016/j.biomaterials.2021.120808. [PubMed: 33895491]
36. Cohrs CM, Panzer JK, Drotar DM, Enos SJ, Kipke N, Chen C, Bozsak R, Schöniger E, Ehehalt F, Distler M, et al. (2020). Dysfunction of Persisting β Cells Is a Key Feature of Early Type 2 Diabetes Pathogenesis. Cell Rep. 31, 107469. 10.1016/j.celrep.2020.03.033. [PubMed: 32268101]
37. Apaolaza PS, Petropoulou P-I, and Rodriguez-Calvo T (2021). Whole-Slide Image Analysis of Human Pancreas Samples to Elucidate the Immunopathogenesis of Type 1 Diabetes Using the QuPath Software. Front. Mol. Biosci. 8, 689799. 10.3389/fmolb.2021.689799. [PubMed: 34179094]
38. Lehrstrand J, Davies WIL, Hahn M, Korsgren O, Alanentalo T, and Ahlgren U (2024). Illuminating the complete ß-cell mass of the human pancreas-signifying a new view on the islets of Langerhans. Nat. Commun. 15, 3318. 10.1038/s41467-024-47686-7. [PubMed: 38632302]
39. Bonifacio E (2015). Predicting Type 1 Diabetes Using Biomarkers. Diabetes Care 38, 989–996. 10.2337/dc15-0101. [PubMed: 25998291]
40. Ziegler AG, Rewers M, Simell O, Simell T, Lempainen J, Steck A, Winkler C, Ilonen J, Veijola R, Knip M, et al. (2013). Seroconversion to Multiple Islet Autoantibodies and Risk of Progression to Diabetes in Children. JAMA 309, 2473–2479. 10.1001/jama.2013.6285. [PubMed: 23780460]
41. Evans-Molina C, Sims EK, DiMeglio LA, Ismail HM, Steck AK, Palmer JP, Krischer JP, Geyer S, Xu P, and Sosenko JM; Type 1 Diabetes TrialNet Study Group (2018). b Cell dysfunction exists more than 5 years before type 1 diabetes diagnosis. JCI Insight 3, e120877. 10.1172/jci.insight.120877. [PubMed: 30089716]
42. Augustine P, Gent R, Louise J, Taranto M, Penno M, Linke R, and Couper JJ; ENDIA Study Group (2020). Pancreas size and exocrine function is decreased in young children with recent-onset Type 1 diabetes. Diabet. Med. 37, 1340–1343. 10.1111/dme.13987. [PubMed: 31094026]
43. Penno MAS, Oakey H, Augustine P, Taranto M, Barry SC, Colman PG, Craig ME, Davis EA, Giles LC, Harris M, et al. (2020). Changes in pancreatic exocrine function in young at-risk children followed to islet autoimmunity and type 1 diabetes in the ENDIA study. Pediatr. Diabetes 21, 945–949. 10.1111/pedi.13056. [PubMed: 32430977]
44. Atkinson MA, and Mirmira RG (2023). The pathogenic “symphony” in type 1 diabetes: A disorder of the immune system, β cells, and exocrine pancreas. Cell Metab. 35, 1500–1518. 10.1016/j.cmet.2023.06.018. [PubMed: 37478842]
45. Legland D, Arganda-Carreras I, and Andrey P (2016). MorphoLibJ: integrated library and plugins for mathematical morphology with ImageJ. Bioinformatics 32, 3532–3534. 10.1093/bioinformatics/btw413. [PubMed: 27412086]

Highlights

- Pancreas tissue slices allow for concurrent investigation of islet and acinar cell secretion
- Islet cell mass, density, and endocrine function are similar across normal human pancreas
- Insulin secretion is impaired across all pancreatic regions with recent-onset T1D
- Near T1D onset, *in situ* acinar cell secretion is preserved across the pancreatic regions

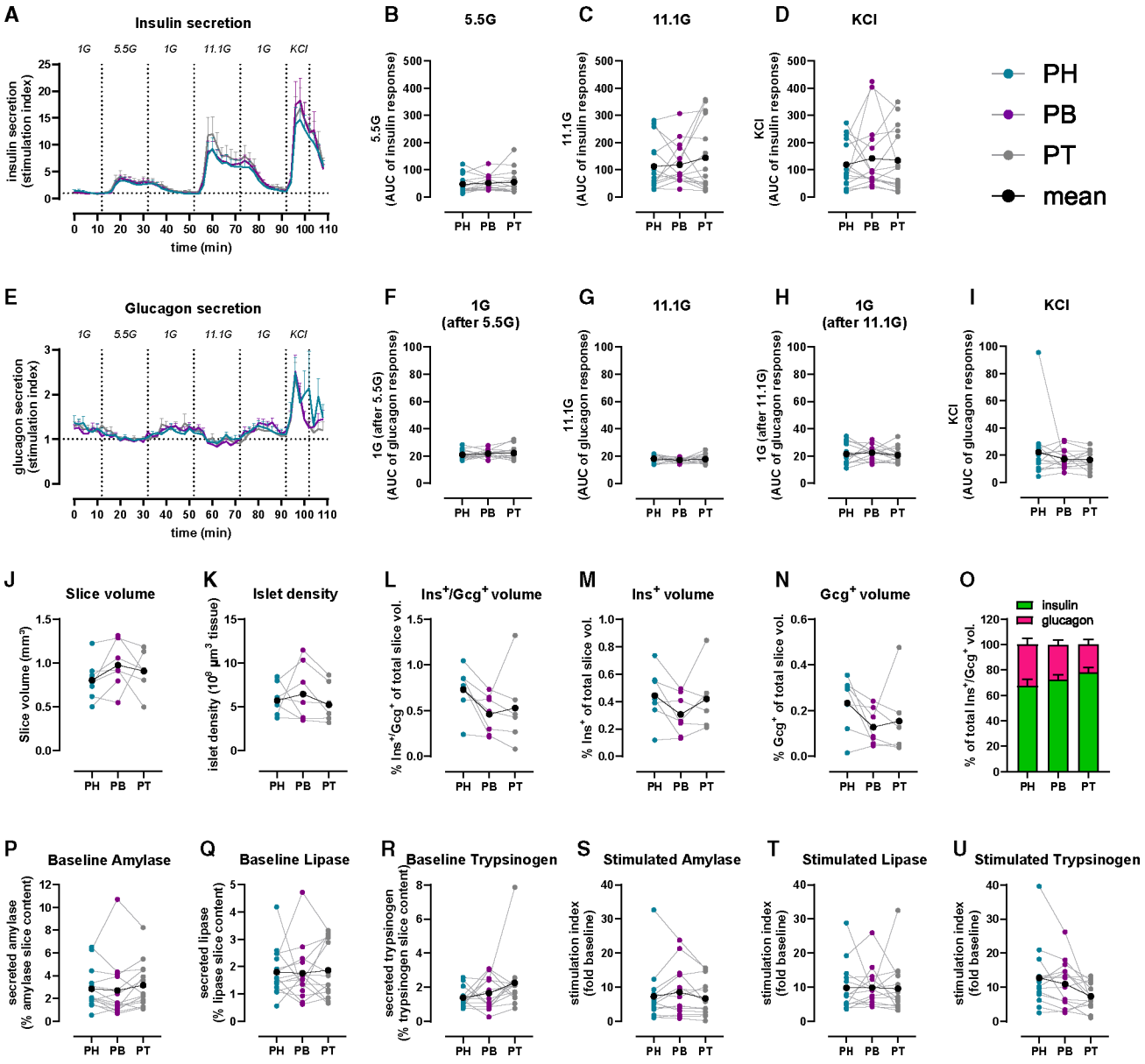

Figure 1. Similar islet and acinar cell secretion across the PH, PB, and PT in ND human pancreas

(A and E) Insulin (A) and glucagon (E) secretion traces from PH (teal), PB (purple), and PT (gray) slices shown as stimulation index (fold of baseline: 1G for insulin, 5.5G for glucagon).

(B–D) Quantification of insulin responses to 5.5G (B), 11.1G (C), and KCl (D).

(F–I) Quantification of glucagon responses to 1G (F), 11.1G (G), 1G (H), and KCl (I).

(J–O) 3D morphometry of perifused slices showing slice volume (J), islet density (K), endocrine (L), insulin (M), and glucagon (N) volumes and the contribution of insulin and glucagon to total endocrine volume (O).

(P–R) Baseline pancreatic amylase (P), lipase (Q), and trypsinogen (R) release expressed as a percentage of total enzyme content.

(S–U) Carbachol-stimulated amylase (S), lipase (T), and trypsinogen (U) secretion expressed as stimulation index (fold of baseline).

n = 15 ND donors (A–I), 7 ND donors (J–O), with 4 slices/region/donor, and 14 ND donors (P–U) with 5 slices/region/donor. Dots represent individual donors with means shown in black. Data are represented as mean ± SEM with repeated measures (RM) one-way ANOVA of log-transformed data.

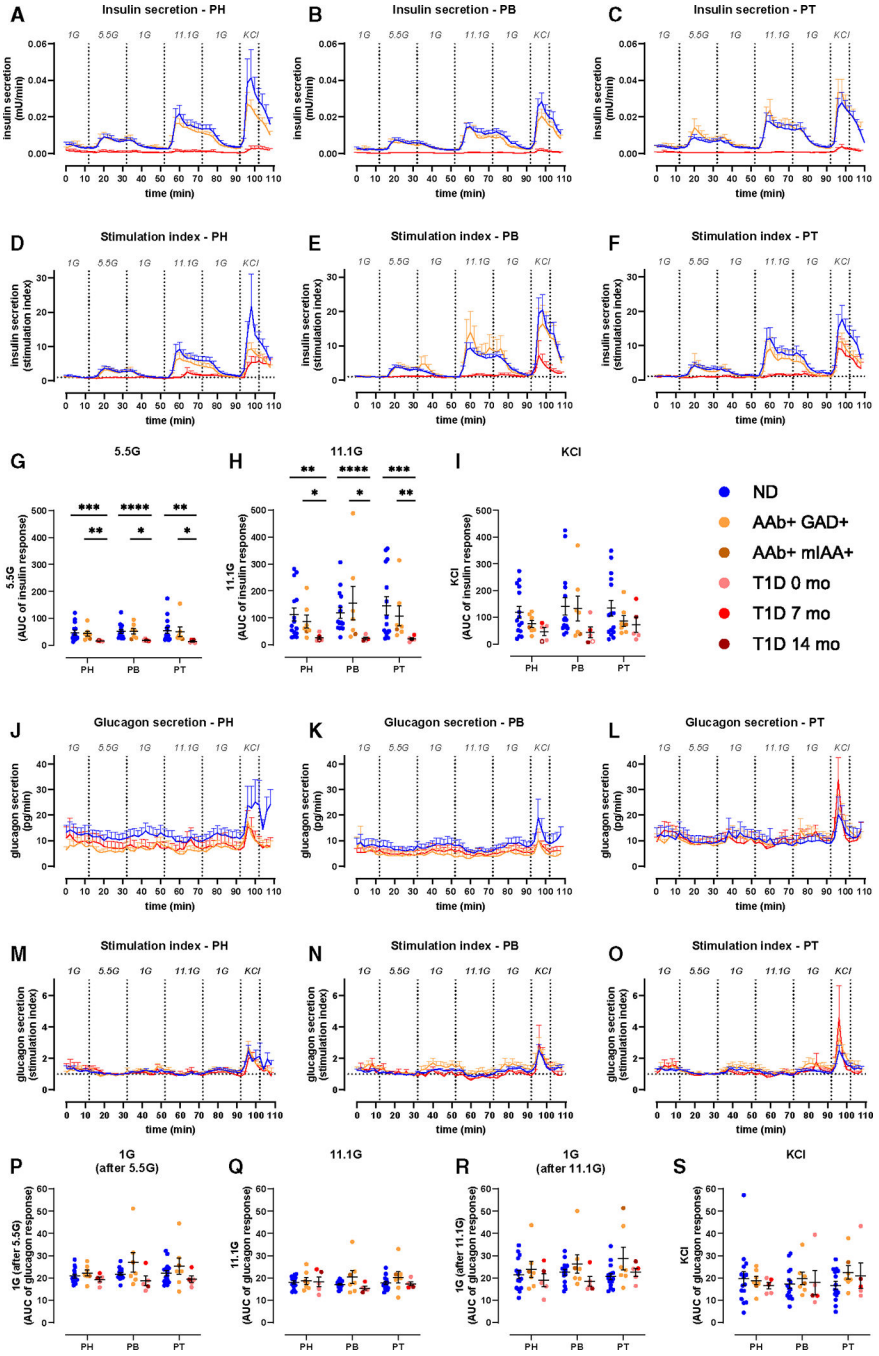

Figure 2. Reduced insulin, but not glucagon secretion in all pancreas regions in recent-onset T1D

(A–C) Insulin secretion from slices of PH (A), PB (B), and PT (C) from ND, 1AAb+, and T1D shown as absolute amounts (mU/min).

(D–F) Insulin secretion traces from slices of PH (D), PB (E), and PT (F) from ND, 1AAb+, and T1D donors shown as stimulation index (fold of 1G baseline).

(G–I) Quantification of insulin responses to 5.5G (G), 11.1G (H), and KCl (I) stimulation.

(J–L) Glucagon secretion from slices of PH (J), PB (K), and PT (L) from ND, 1AAb+, and T1D shown as absolute amounts (pg/min).

(M–O) Glucagon secretion traces from slices of PH (M), PB (N), and PT (O) from ND, 1AAb+, and T1D donors shown as stimulation index (fold of 5.5G baseline).
(P–S) Quantification of glucagon responses to 1G (P), 11.1G (Q), 1G (R), and KCl (S). n = 15 ND, 7 1AAb+, and 5 T1D donors with 4 slices/region/donor. Dots represent individual donors shown with mean ± SEM and RM two-way ANOVA of log-transformed data. *$p < 0.05$, **$p < 0.01$, ***$p < 0.001$, and ****$p < 0.0001$.
See also Figures S2 and S3.

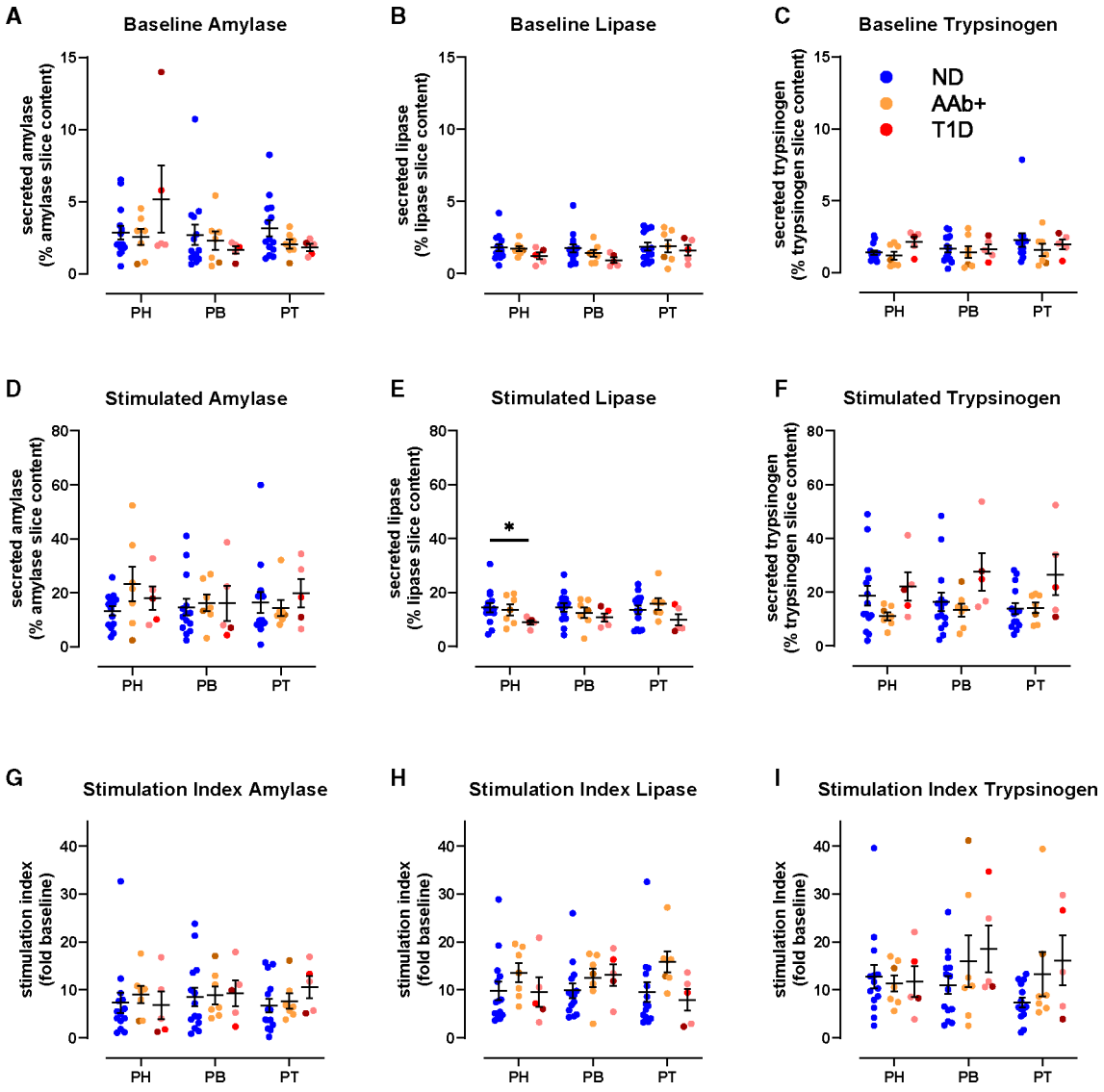

Figure 3. Preserved acinar cell function at T1D onset

(A–C) Baseline pancreatic amylase (A), lipase (B), and trypsinogen (C) release in ND, 1AAb+, and T1D slices from PH, PB, and PT expressed as a percentage of total enzyme content.

(D–F) Carbachol-stimulated amylase (D), lipase (E), and trypsinogen (F) secretion in ND, 1AAb+, and T1D slices from PH, PB, and PT expressed as a percentage of total enzyme content.

(G–I) Carbachol-stimulated amylase (G), lipase (H), and trypsinogen (I) secretion in ND, 1AAb+, and T1D slices from PH, PB, and PT expressed as stimulation index (fold of baseline).

n = 14 ND, 7 1AAb+, and 5 T1D donors with 5 slices/region/donor. Dots represent individual donors shown with mean ± SEM and RM two-way ANOVA. *$p < 0.05$.

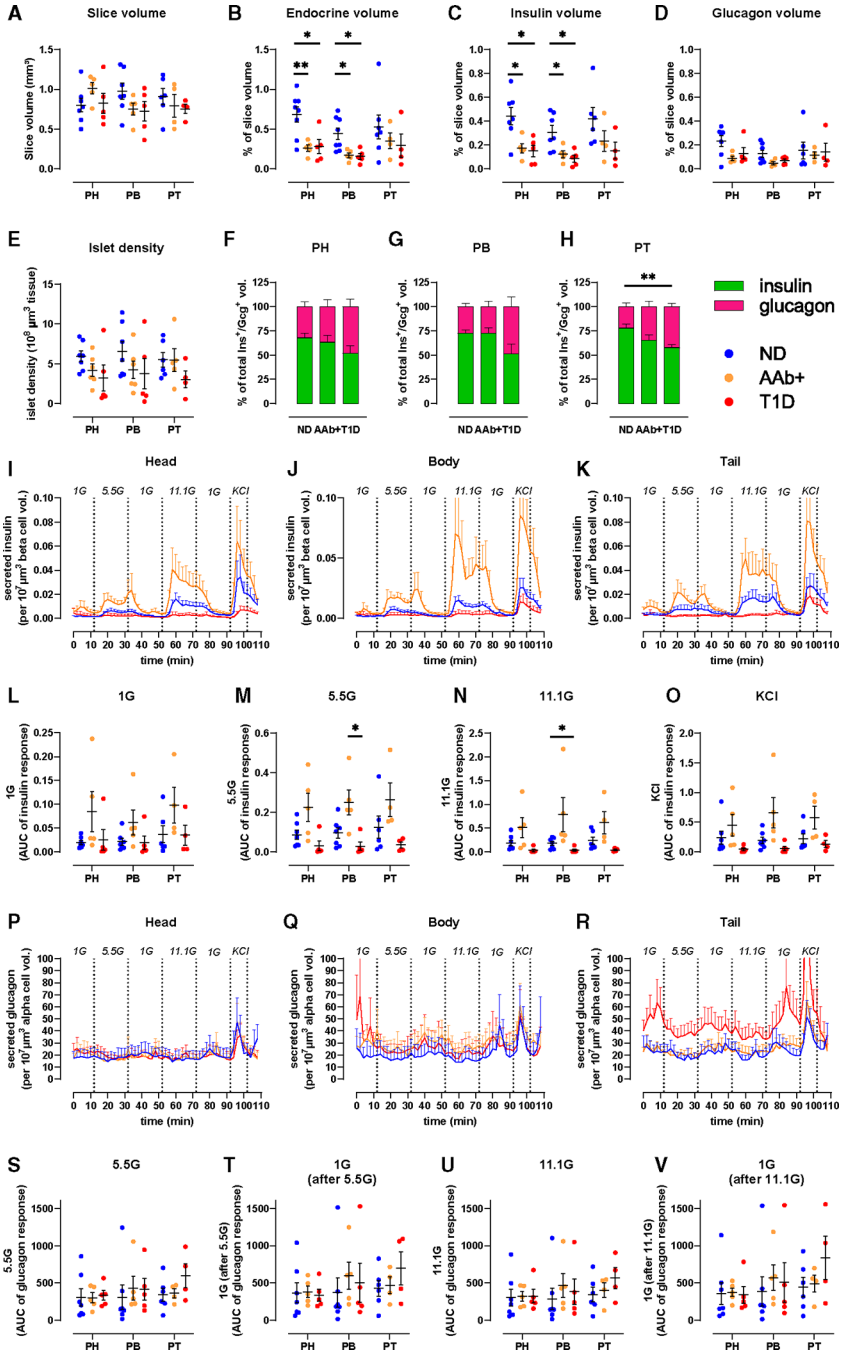

Figure 4. Decreased endocrine and beta-cell mass across the pancreas at T1D onset

(A–H) 3D morphometry of perifused slices showing whole-slice (A), endocrine (B), insulin (C), and glucagon (D) volumes, islet density (E), and the contributions of insulin and glucagon to total endocrine volume across disease groups in PH (F), PB (G), and PT (H).

(I–K) Insulin secretion traces from slices of PH (I), PB (J), and PT (K) from ND, 1AAb+, and T1D shown as secreted insulin normalized to respective beta-cell volume.

(L–O) Quantification of insulin responses to 1G (L), 5.5G (M), 11.1G (N), and KCl (O).

(P–R) Glucagon secretion traces from slices of PH (P), PB (Q), and PT (R) from ND, 1AAb+, and T1D shown as secreted glucagon normalized to respective alpha-cell volume. (S–V) Quantification of glucagon responses to 5.5G (S), 1G (T), 11.1G (U), and 1G (V). $n = 7$ ND, 5 1AAb+, and 5 T1D donors with 4 slices/region/donor. Dots represent individual donors with mean ± SEM and RM two-way ANOVA of log-transformed data. *$p < 0.05$ and **$p < 0.01$.

See also Figure S4.

KEY RESOURCES TABLE

REAGENT or RESOURCE	SOURCE	IDENTIFIER
Antibodies		
Polyclonal Guinea Pig Anti-Insulin	Agilent - Dako	Cat# IR00261–2; RRID: AB_2800361
Monoclonal Mouse Anti-Glucagon	Sigma-Aldrich	Cat# G2654; RRID: AB_259852
AlexaFluor® 488 Goat Anti-Guinea Pig	Thermo Fisher Scientific - Invitrogen	Cat# A-11073; RRID: AB_2534117
AlexaFluor® 633 Goat Anti-Mouse	Thermo Fisher Scientific - Invitrogen	Cat# A-21050; RRID: AB_2535718
Biological samples		
Human Pancreas Tissue	nPOD;https://npod.org/	RRID: SCR_014641
nPOD-6540		RRID: SAMN25652251
nPOD-6543		RRID: SAMN25652254
nPOD-6544		RRID: SAMN25652255
nPOD-6546		RRID: SAMN25652257
nPOD-6547		RRID: SAMN25652258
nPOD-6548		RRID: SAMN25652259
nPOD-6550		RRID: SAMN25652261
nPOD-6551		RRID: SAMN25652262
nPOD-6552		RRID: SAMN30386842
nPOD-6553		RRID: SAMN30386843
nPOD-6556		RRID: SAMN30386845
nPOD-6558		RRID: SAMN30386847
nPOD-6559		RRID: SAMN30386848
nPOD-6560		RRID: SAMN30386849
nPOD-6562		RRID: SAMN30386850
nPOD-6563		RRID: SAMN30386851
nPOD-6569		RRID: SAMN38117299
nPOD-6571		RRID: SAMN33284289
nPOD-6573		RRID: SAMN33284291
nPOD-6575		RRID: SAMN33284293
nPOD-6578		RRID: SAMN33284295
nPOD-6579		RRID: SAMN33284296
nPOD-6582		RRID: SAMN38117302
nPOD-6583		RRID: SAMN38117303
nPOD-6584		RRID: SAMN38117304
nPOD-6586		RRID: SAMN38117306
nPOD-CV14		RRID: SAMN38117313
Chemicals, peptides, and recombinant proteins		
Aprotinin	MilliporeSigma	Cat# A6106
Low Melting Point Agarose	MilliporeSigma	Cat# A0701

REAGENT or RESOURCE	SOURCE	IDENTIFIER
Low Glucose DMEM	MilliporeSigma	Cat# D6046
Fetal Bovine Serum	Cytiva	Cat# SH30071.03IH
Antibiotic-Antimycotic Solution	Corning	Cat# 30–004-CI
DMEM (Powder)	Corning	Cat# MT9013PB
Sodium Pyruvate	MilliporeSigma	Cat# P2256
HEPES	MilliporeSigma	Cat# H4034
L-Glutamine	Thermo Fisher	Cat# 25030081
Bovine Serum Albumin	MilliporeSigma	Cat# A6003
Carbamylcholine chloride	MilliporeSigma	Cat# C4382
Triton X-100	MilliporeSigma	Cat# 648462
4% Paraformaldehyde	Thermo Fisher Scientific	Cat# J19943.K2
PBS with Azide	Santa Cruz Biotechnology	Cat# SC-296028
DAPI	Sigma-Aldrich	Cat# D9542
Critical commercial assays		
Insulin ELISA Kit	Mercodia	Cat# 10-1113-10
Ultrasensitive Insulin ELISA	Mercodia	Cat# 10-1132-01
Glucagon ELISA Kit	Crystal Chem	Cat# 81520
Human Pancreatic Amylase ELISA Kit	Abcam	Cat# ab137969
Human Pancreatic Lipase ELISA Kit	Novus Biologicals	Cat# NB016815
Trypsin RIA	ALPCO	Cat# 72-OCFE07-TRYPS
Software and algorithms		
Prism 9.4.0	GraphPad	RRID: SCR_002798
ImageJ	https://imagej.nih.gov/ij/	RRID:SCR_003070
MorphoLibJ	https://imagej.net/plugins/morpholibj	N/A
FIJI	https://imagej.net/software/fiji/	RRID:SCR_002285
Las X Life Science Microscope Software Platform	https://www.leica-microsystems.com/products/microscope-software/p/leica-las-x-ls/	RRID:SCR_013673
Other		
Perifusion System	Biorep Technologies	Cat#PERI4–115
Semiautomatic Vibratome VT1200S	Leica	Cat#14048142065
Perifusion Chamber	Warner Instruments	Cat#64–0223
Perifusion Platform	Warner Instruments	Cat#64–0281 [P-5]
Laser Scanning Confocal Microscope	Leica	Model: TCS SP8 SMD